TRENDS IN SCIENCES 2026; 23(1): 11091
https://doi.org/10.48048/tis.2026.11091 RESEARCH ARTICLE

Effect of Differential Oxidation of LDL on Foam Cell Formation and Expression of MMP-9 and CD147 in PMA-Derived Macrophage Foam Cells

Kanokwan Lowhalidanon[2], Warapan Panchai[1] and Panida Khunkaewla[1,*]

[1]*Biochemistry-Electrochemistry Research Unit, School of Chemistry, Institute of Science, Suranaree University of Technology, Nakhon Ratchasima 30000, Thailand*
[2]*Institute of Medicine, Suranaree University of Technology, Nakhon Ratchasima 30000, Thailand*

([*]Corresponding author's e-mail: kpanida@sut.ac.th)

Received: 27 June 2025, Revised: 30 July 2025, Accepted: 6 August 2025, Published: 20 October 2025

Abstract

High plasma low-density lipoprotein (LDL) levels can trigger phagocytosis of macrophages to become foam cells that can initiate atherosclerosis progression. LDL undergoes stepwise oxidation to minimally modified LDL (mm-LDL) and fully oxidized LDL (ox-LDL). This study investigated the effect of LDL with different degrees of oxidation, including LDL, mm-LDL and ox-LDL, on foam cell formation and expression of MMP-9 and CD147 in macrophages. Phorbol 12-myristate 13-acetate-derived macrophages from U937 cells were used as the study model. Cells were co-cultivated with or without different types of LDL at various concentrations and times before characterization. The results revealed that LDL induced the strongest intracellular lipid response, with conversion of macrophages to foam cells. Upregulation of CD36, but not of LDL receptors, was observed on incubation with all types of LDL, suggesting its role in the endocytosis of the studied LDLs. Upregulation of MMP-9 in foam cells was observed both in cell lysates and in the secreted form after 48 h of cultivation. MMP-9 conversion from pro-form to active form was detected after 72 h of cultivation with all types of LDL, but most strongly with LDL and ox-LDL, and was correlated with the upregulation of membrane-bound CD147 (mCD147). In summary, this study indicates that different degrees of LDL oxidation induced different severities of foam cell formation, induction of MMP-9 and mCD147.

Keywords: Minimally modified-LDL (mm-LDL), Fully oxidized-LDL (ox-LDL), Foam cell, MMP-9, CD36, CD147

Introduction

The initiation hallmark of atherosclerosis development is the formation of foam cells in the arterial intima. High levels of plasma LDL can cause the translocation of these particles across the arterial cell wall to the intima, and some then undergo molecular modifications such as oxidation and can be phagocytosed by macrophages, leading to the accumulation of free cholesterol in the cytoplasm and conversion to foam cells [1-3]. LDL can be oxidized in a stepwise manner, resulting in different degrees of oxidation. The initial phase of modification is the reaction of lipid components with oxidizing agents, resulting in radical chain reactions that produce several oxidation products, known as minimally modified low density lipoprotein (mm-LDL). During prolonged oxidation, apo-B100 in LDL is attacked by lipid oxidation products, leading to the oxidation of amino acid side-chains and the cleavage of peptide bonds. The product in which both lipid and protein components are modified is called fully oxidized-LDL (ox-LDL) [4-6].

LDLs are phagocytosed by macrophages to become foam cells, via their surface receptors. Native LDL was uptaken mainly via LDL receptors (LDL-R), while mm-LDL and ox-LDL are taken up via scavenger receptors (SRs) type B, also known as CD36, a highly glycosylated protein of molecular weight 88 kDa that was reported to be expressed in multiple cell types, including macrophages [7-11]. The CD36 molecule

plays a central role in macrophage-to-foam cell transformation, positioning it as a promising target for inhibition strategies [12-14]. Several *in vitro* studies of foam cell formation have utilized U937 monocytes, which can be differentiated into macrophage-like cells by stimulation with phorbol 12-myristate 13-acetate (PMA) [15]. Complete differentiation into macrophages is marked by distinct morphological changes, transitioning from suspension growth to adherent behavior with pseudopodia formation, along with upregulated expression of the surface markers CD14 and CD45 [15]. Furthermore, PMA-differentiated macrophages exhibit upregulated expression of CD36, supporting its role in foam cell formation and lipid metabolism [16].

Atherosclerosis is a progressive inflammatory disease initiated by increased foam cell accumulation at the arterial wall as the plaques grow and local inflammation through chemokines, cytokines and reactive-oxygen species (ROS) occurs [17,18]. The stability of the plaques depends on dynamic interactions between extracellular matrix (ECM) components such as fibrinogen and collagen around the fibrous cap, and their degradation by matrix metalloproteinases (MMPs). Stable plaques are typically characterized by a thick fibrous cap rich in ECM proteins such as collagen, while unstable plaques exhibit extensive ECM degradation, cap thinning and increased risk of rupture. Therefore, the dynamic balance between ECM production and degradation - primarily mediated by MMPs - plays a pivotal role in determining plaque vulnerability [19]. Expression of several MMPs is reportedly induced by the extracellular matrix metalloproteinase inducer (EMMPRIN), also known as CD147. Ox-LDL can stimulate CD147 expression on macrophages and coronary smooth muscle cells, leading to induction of MMP-9 expression in human macrophages, which affects the stability of atherosclerotic plaques [20-22].

As mentioned above, extensive research has highlighted ox-LDL as a critical factor in promoting foam cell formation and in modulating the expression of MMPs, including MMP-9, as well as CD147. Despite these findings, the differential impact of varying oxidation levels of LDL on foam cell generation and the interplay between MMP-9 and CD147 expression in macrophage-derived foam cells has not been compared. Accordingly, this study aimed to evaluate the effects of distinct LDL oxidation on foam cell formation and the expression of MMP-9 and its inducing molecule CD147 in macrophages. Here we provide promising evidence that LDL particles with different degrees of oxidation have different capacities to form foam cells, in a dose- and time-dependent manner. These differences reflect the different levels of MMP-9 and CD147 expression on macrophage foam cells produced by non-oxidized LDL and ox-LDL.

Materials and methods

Cells

Macrophages were differentiated by stimulation of cell line U937 with phorbol 12-myristate 13-acetate (PMA) in a procedure adapted from previous reports [23]. Briefly, U937 cells (1×10^6 cells) were seeded in 6-well plates and cultured in RPMI 1640 medium (Gibco, USA) supplemented with 10% fetal bovine serum (FBS) (Gibco). PMA (Sigma-Aldrich, USA) was added to a final concentration of 100 ng/mL and cultivation continued for 48 h at 37 °C in a 5% CO_2 incubator. The culture supernatant was discarded, and the adherent differentiated cells were washed twice with RPMI 1640 medium and re-cultured in Optimem® serum-free medium (Gibco) for further experiments.

Antibodies

Anti-CD14 monoclonal antibody (mAb) clone MT14/1 (IgG1) and anti-CD45 mAb clone MT45 (IgG1) were kindly provided by Prof. Dr. Watchara Kasinrerk, Chiang Mai University, Thailand. Anti-human LDL receptor mAb clone 2H7.1 (IgG2b) was purchased from Merck (Darmstadt, Germany). Anti-CD36 mAb clone TR9 (IgG1) was from ImmunoTools (Friesoythe, Germany). Anti-CD147 mAb clone MEM-M6/6 (IgG1) was from EXBIO (Vestec u Prahy, Czech Republic). Anti-human LDL mAbs clone hLDL-E8 (IgG1) and hLDL-2D8 (IgG2b) were generated in house [5,24]. Alexa Fluor 488-conjugated goat-anti-mouse IgG (AF488-anti-mouse IgG) and anti-human MMP-9 mAb (IgG2a) were from Thermo Scientific (USA). Horseradish Peroxidase (HRP)-conjugated rabbit-anti-mouse immunoglobulins antibodies (HRP-anti-mIgs) were from Dako (Glostrup, Denmark). Anti-beta actin mAb (IgG1) was from BioRad (USA).

LDL preparation

LDL was precipitated from human plasma using heparin-citrate as previously reported [5]. The precipitated LDL was dissolved in 1× phosphate buffered saline (PBS) pH 7.2 of the same volume as the original plasma. For LDL oxidation, human LDL (final concentration 1 mg/mL) was incubated with 10 μM $CuSO_4$ in PBS at 37 °C for either 9 or 48 h, generating mm-LDL or ox-LDL, respectively. A reagent blank was prepared by incubation of 10 μM $CuSO_4$ in PBS at 37 °C for 48 h. The degree of oxidation of LDL was evaluated by a thiobarbituric acid-reactive substances (TBARS) assay and indirect ELISA using in-house generated anti-human LDL mAb (**Figure S1**). All types of LDL were kept at 4 °C for further experiments and sterilized by filtration through 0.22 μm filter paper before use.

Immunofluorescence staining and flow cytometry

Macrophages (1×10^7 cells/mL) suspended in staining buffer (1% BSA in PBS containing 0.02% sodium azide) were pre-incubated with human IgG (2 μg/mL) for 30 min at 4 °C. Fifty microliters of anti-CD14 mAb (dilution 1:100), anti-CD45 mAb (5 μg/mL), anti-LDL-R mAb (20 μg/mL), anti-CD36 mAb (5 μg/mL), anti-CD147 mAb (5 μg/mL) or isotype-matched control was added to an equal volume of cell suspension. After incubation at 4 °C for 30 min, the stained cells were washed twice with staining buffer and incubated with AF488-anti-mouse IgG at a final dilution of 1:1,000 in staining buffer for another 30 min at 4 °C. The stained cells were washed 3 times with staining buffer and analysed in a flow cytometer (BD Bioscience). The relative mean fluorescence intensity (rMFI) was calculated from histogram data (**Figures S2 - S4**) according to Eq. (1).

$$rMFI = \frac{Geo\ mean\ of\ test - Geo\ mean\ of\ conjugated\ control}{Geo\ mean\ of\ macrophage\ (or\ macrophage\ with\ reagent\ blank^{*}) - Geo\ mean\ of\ conjugate} \quad (1)$$

*Macrophages incubated with LDL were normalized to macrophages incubated in media. Macrophages incubated with mm-LDL or ox-LDL were normalized to macrophages incubated with the reagent blank.

Cholesterol concentration determination by colorimetry

Macrophages were gently rinsed twice with PBS. One milliliter of the lipid extraction solvent, hexane: Isopropanol (3:2), was added into the dried cells in a 6-well plate, mixed well and placed at RT in a fume hood to allow evaporation of extracting solvent. Five hundred microliters of cholesterol CHOD/PAP monoreagent (Centronic GmbH, Germany) was added, thoroughly mixed, and transferred to a 1.5 mL tube. After incubation at 37 °C for 5 min, the absorbance of the colored-end product was measured at 505 nm. The cholesterol concentration was calculated from the standard curve.

First strand cDNA synthesis

Total RNA was extracted from macrophages using GENEzol™ reagent (Geneaid, Taiwan) according to the manufacturer's guidelines. The purity and concentration of extracted RNA were evaluated using a NanoDrop spectrophotometer (Thermo Scientific, USA). The A_{260}/A_{280} and A_{260}/A_{230} absorbance ratios ranged from 1.9 to 2.0, indicating high purity of the RNA and its suitability for downstream applications. RNA concentration was determined by measuring absorbance at 260 nm, applying the standard conversion factor of 1 A_{260} = 40 μg/mL of RNA. The extracted RNA was used for first-strand cDNA synthesis using a Viva cDNA synthesis kit (Vivantis, Malaysia) according to the manufacturer's instructions. Briefly, cDNA synthesis was performed in a 20 μL reaction mixture containing 1 μg of RNA extract, 50 ng of oligo dT primer, 1 mM dNTPs and nuclease-free water (10 μL). Incubation at 65 °C for 5 min was followed by chilling on ice for 2 min. The RNA-primer mixture was then mixed with 10 μL of cDNA synthesis mix (100 units of M-MuLV reverse transcriptase in 2 μL of 10X Buffer M-MuLV, topped up with nuclease-free water). The RT-PCR reaction was carried out by incubating samples at 42 °C for 60 min and the reaction was terminated by denaturation of residual reverse transcriptase at 85 °C for 5 min. The synthesized cDNA was kept at –80 °C until used. The cDNA concentration used in subsequent experiments was determined by the initial RNA input for cDNA synthesis.

Semi-quantitative real-time polymerase chain reaction (qPCR)

The PCR amplification reaction mixture (20 µL) contained 50 ng of cDNA, 250 nM forward and reverse primers specific for the MMP-9 gene and the reference gene ACTB (**Table 1**) and 10 µL of 2X LightCycler® 480 SYBR green I master mix containing FastStart Taq DNA polymerase (Roche Diagnostics, Germany). The PCR program involved initial denaturation at 95 °C for 10 s, primer annealing at 59 °C for 15 s and extension at 72 °C for 20 s. For melting curve analysis, the reaction was run for a cycle of 5 s and 1 min at 95 and 65 °C, respectively. The relative mRNA quantification of target genes was conducted according to 2^(-ΔΔCT) method. Reference gene ACTB transcripts were used for normalization and quality control.

Table 1 Specific primers used for RT-PCR amplification (BioDesign, Thailand).

Sequence name		Sequence (5' → 3')	Fragment (bp)
MMP-9	Forward	CTC-TGG-AGG-TTC-GAC-GTG-AA	120
	Reverse	GGC-TTT-CTC-TCG-GTA-CTG-GA	
ACTB	Forward	TCA-TGA-AGT-GTG-ACG-TGG-ACA-TC	151
	Reverse	GGA-GCA-ATG-ATC-TTG-ATC-TTC-AT	

Cell lysate preparation

Macrophages (1×10^7 cells) were harvested and washed 3 times with 1× PBS pH 7.2. The cells were solubilized for 30 min on ice in 1 mL of lysis buffer (1% Triton X-100, 50 mM Tris-HCl pH 7.5, 150 mM NaCl, 2 mM EDTA, 1 mM phenylmethylsulfonyl fluoride (PMSF), 2 µM pepstatin A, 10 µg/mL aprotinin and 5 mM iodoacetamide). Clear cell lysates were obtained by centrifugation at 14,000 rpm at 4 °C for 10 min and were kept on ice before use.

Western blotting

Ten micrograms of proteins in culture supernatant or cell lysates were resolved by 10% SDS-PAGE under reducing conditions and electrophoretically transferred onto a polyvinylidenefluoride (PVDF) membrane. The membrane was blocked with 5% skimmed milk in PBS at RT for 1 h before incubation with either anti-human MMP-9 mAb at dilution 1:2000 or anti-beta actin mAb at dilution 1:40000 in 2.5% skimmed milk in PBS at RT on a rocker shaker for 1 h. The stained membranes were washed 5 times with 0.1% Tween-20 in PBS (PBST) before incubation with HRP-anti-mIgs at dilution 1:5000 in 2.5% skimmed milk in PBS for an hour at RT. After thorough washing 3 times with PBST and twice with PBS, protein bands were visualized using an enhanced chemiluminescent detection system (SuperSignal™ West Pico PLUS; Thermo Scientific).

Gelatin zymography

Six micrograms of protein in culture supernatant or 100 µg of cell lysate protein were electro-separated using 10% SDS-PAGE containing 0.1% gelatin (Sigma Aldrich). After electrophoresis, the gel was washed with renaturing buffer contained 2.5% Triton®X-100 for 40 min at RT to remove SDS and subsequently incubated with activating buffer (50 mM Tris-HCl, 0.15 M NaCl and 10 mM $CaCl_2$) at 37 °C for 16 h. The activated gel was stained in 0.025% Coomassie Brilliant Blue R-250 (Applichem, Germany) for 30 min at RT and de-stained for another 30 min. The pro- and active-form of MMP-9 (gelatinase B) were observed as digested clear bands on the gel.

Statistical analysis

Statistical analysis was carried out using GraphPad Prism 9.0 (GraphPad Software, Inc., San Diego, CA). Descriptive data and results are presented as means ± SD. Data analysis was performed by unpaired t-test and one-way ANOVA. Results were considered significant if $p < 0.05$ (***, $p < 0.001$; **, $p < 0.01$; *, $p < 0.05$).

Results and discussion

PMA-derived macrophages express cell surface CD36, but not LDL receptor.

Macrophages were differentiated from U937 cells by activation with PMA. The generated cells were transformed from a suspension to adherent cells with

pseudopodia (**Figure 1(A)**). Complete differentiation of U937 cells to macrophages was confirmed by cell surface staining of the macrophage cell markers including CD14 and CD45 [15] and analyzed by flow cytometry. According to the results shown in **Figure 1(B)**, both cell surface markers were upregulated in PMA-activated cells compared to the original U937 cells, indicating that the differentiation of U937 into macrophages could be used as a model in this study. Furthermore, the expression of receptors for LDL uptake was investigated and it was found that CD36, a class B scavenger receptor, but not LDL-R, was up-regulated on the cell surface of the generated macrophages, compared with the isotype control (**Figure 1(B)**).

LDL, mm-LDL and ox-LDL induced different severity of foam cell formation

As the major component of LDL particles is cholesterol, the internalization of LDL by PMA-derived macrophages to become foam cells can be evaluated by examination of the intracellular cholesterol concentration after co-cultivation with different types of LDL. The effect of different oxidative states of LDL on foam cell formation was investigated by co-cultivation of PMA-derived macrophages with various concentrations of LDL, mm-LDL or ox-LDL for different times. Intracellular cholesterol in macrophage foam cells was quantified and found that the intracellular cholesterol concentration of PMA-derived macrophages incubated with all types of LDL increased in a time-dependent manner compared to reagent blank and media controls, with a significant increase after 72 h of incubation.

Total cholesterol concentration in cells incubated with LDL was higher than in those incubated with mm-LDL and ox-LDL, particularly at high concentrations of LDL, starting at 48 h of incubation and reaching the highest concentration at 72 h (**Figure 2**). The highest cholesterol concentration was found in cells that were co-cultivated with LDL, compared to those treated with mm-LDL and ox-LDL. According to our findings, the macrophages generated in this study have no LDL-R on their surface, however it turned out that most intracellular lipid and cholesterol accumulation is induced by native LDL rather than by either mm-LDL or ox-LDL. These results indicate that entry of LDL into the cell is not via LDL receptors but by other routes. For example, it has been reported that LDL can enter the cells by macro- or pinocytosis or via the scavenger receptor CD36, as well as via LDL receptors [10,25].

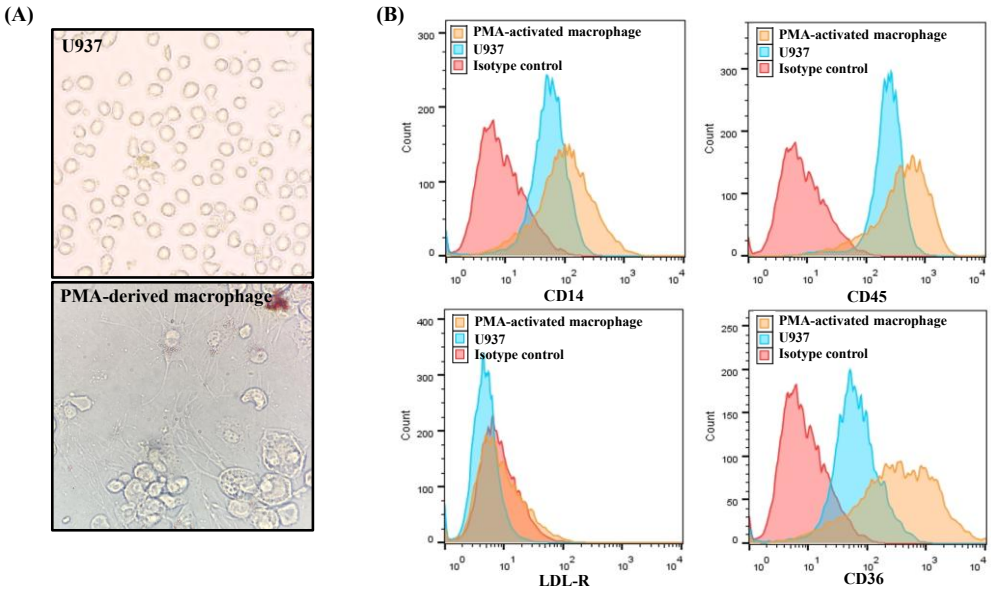

Figure 1 (A) Morphology of U937 cells and PMA-derived macrophages with pseudopodia formation. (B) FACs profiles showed up-regulation of cell surface expression CD14, CD45 and CD36 but not LDL-R on PMA-derived macrophages compared to U937. A representative result from one of 3 independent experiments is shown.

LDL and ox-LDL upregulated cell surface expression of CD36 on macrophage foam cells

As previous experiments showed different degrees of endocytosis into macrophages of different types of LDL, endocytic efficiency thus may depend on the expression of these receptors on the macrophage cell surface. The cell surface expression of LDL-R and the scavenger receptor CD36 on macrophages, on co-cultivation with different types of LDL, was therefore investigated. Immunofluorescence staining and flow cytometry analysis, compared to an isotype-negative control, revealed that mm-LDL and ox-LDL at 100 µg/mL slightly upregulated the expression of LDL-R at 24 h of co-cultivation, while longer incubation of all LDL types had no effect on the expression of LDL-R. Interestingly, the greatest upregulation of LDL-R was found on incubating the macrophages with mm-LDL, final concentration 200 µg/mL, for 24 h (**Figure 3(A)**). In contrast, upregulation of cell surface CD36 expression was induced by all types of LDL and was significant after co-cultivation with either LDL or ox-LDL for 24 h compared to the control (**Figure 3(B)**). According to these results, CD36 provides an endocytic route for all types of LDL, though mainly LDL and ox-LDL rather than LDL-R, in the studied macrophages. Significant upregulation was observed after 24 h of cultivation with either LDL or ox-LDL (**Figure 3(B)**). However, cell surface expression of this molecule varied after 48 and 72 h. Because CD36 is expressed not only on the plasma membrane but also in intracellular compartments there may be recycling between endosomes and the plasma membrane during endocytosis [14,16]. Furthermore, CD36 is known to be a scavenger receptor that can recognize and internalize both LDL and ox-LDL [10,26]. Therefore, variation of CD36 expression on the macrophage foam cells at both 48 and 72 h may be caused by the recycling of CD36 during LDL/ox-LDL recognition and internalization into the cells. Macrophage exposure to mm-LDL, in contrast to native LDL and ox-LDL, induced a slight upregulation of LDL-R expression (**Figure 3(A)**). This result aligns with the upregulation of CD36 expression following mm-LDL treatment, suggesting that mm-LDL may enter macrophages through the CD36 receptor, and the negative feedback mechanism may not be affected by mm-LDL induction, leading to the slight up-regulation of LDL-R.

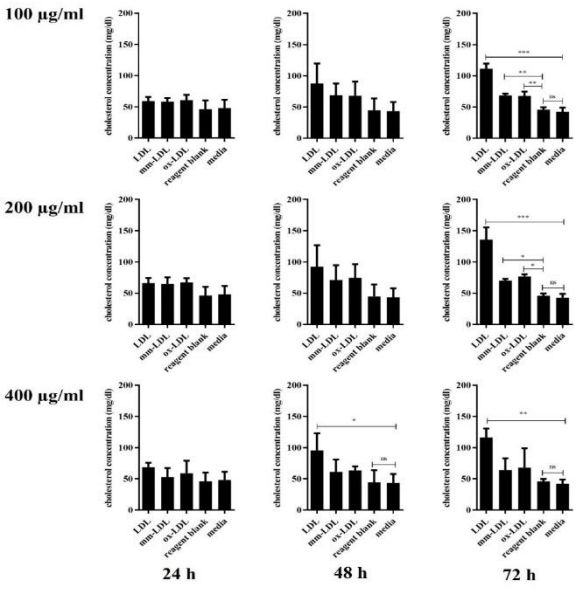

Figure 2 Intracellular cholesterol concentration. PMA-derived macrophages were incubated without or with different types of LDL at various concentrations and times. The cholesterol concentration was determined by an enzymic colorimetric method. Cholesterol concentration in cells incubated with LDL was higher than in those incubated with mm-LDL and ox-LDL, particularly LDL at concentrations at 400 µg/mL, starting at 48 h of incubation and reaching the highest concentration at 72 h. The data represent the means ± SD of 3 independent experiments (ns indicates not significant, * indicates $p < 0.05$, ** indicates $p < 0.01$ and *** indicates $p < 0.001$).

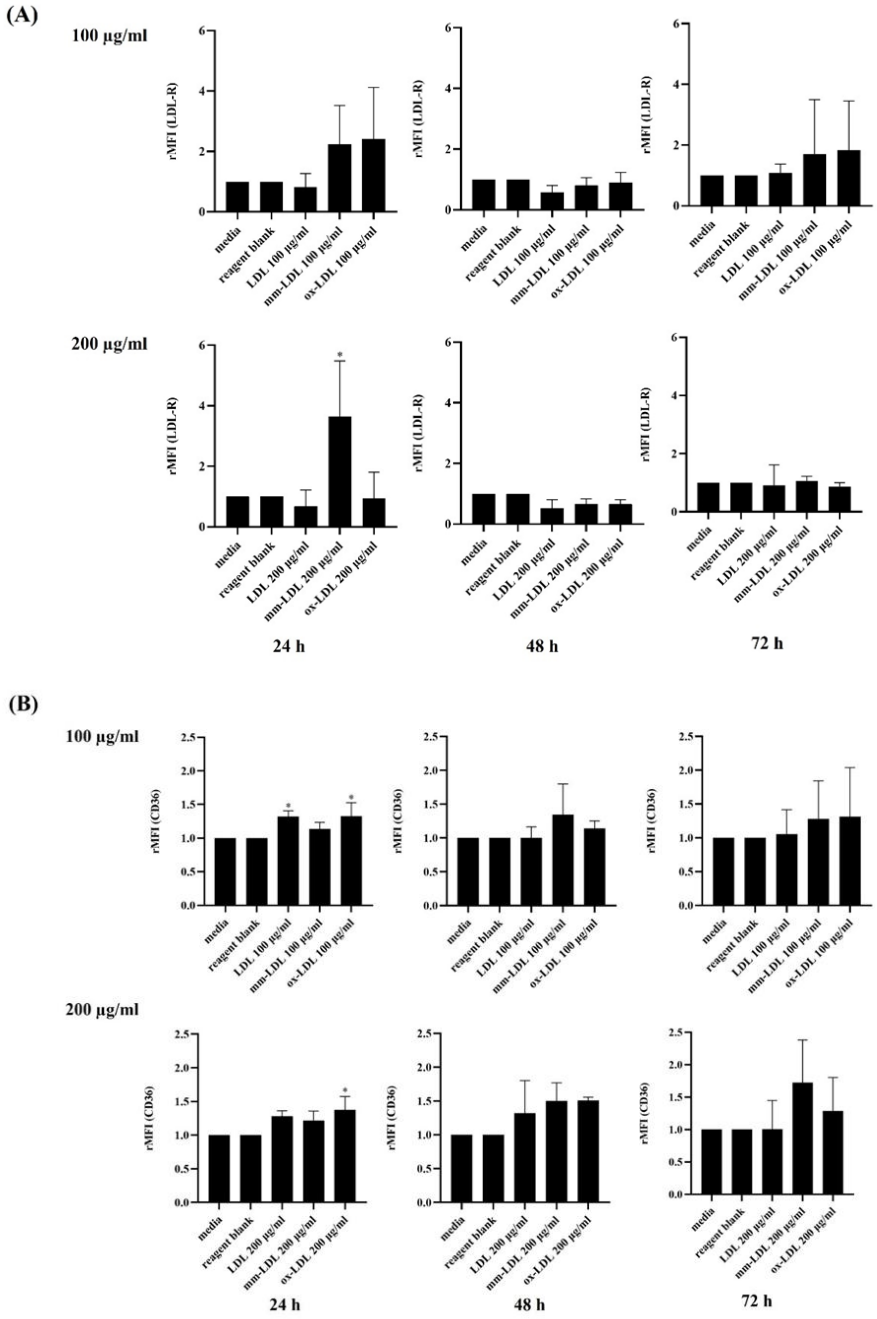

Figure 3 Cell-surface expression of LDL-R and CD36. PMA-derived macrophages were cultivated without or with LDL, mm-LDL or ox-LDL at various concentrations and times. The cells were subjected to indirect immunofluorescence staining and flow cytometry analysis. Expression levels are shown as relative mean fluorescence intensities (rMFI) of LDL-R (A) and CD36 (B). Cultivation of macrophages with mm-LDL at 200 µg /mL caused upregulation of LDL-R, while significant upregulation of CD36 was observed after 24 h of cultivation with either LDL or ox-LDL. The data represent the means ± SD of 3 independent experiments (* indicates $p < 0.05$).

Different degrees of oxidation of LDL induced different levels of MMP-9 expression in PMA-derived macrophages

MMP-9, or gelatinase B, has been shown to be involved in the stability of atherosclerotic plaques in the advanced stage of atherosclerosis [27,28]. MMP-9 was found in the atherosclerotic plaque area, where accumulation of foam cells caused digestion of the extracellular matrix, leading to plaque instability [28,29]. Here we examined whether different degrees of oxidation of LDL had any effect on the expression and activity of this enzyme. Semi-quantitative reverse

transcriptase (RT-PCR) studies revealed that the gene expression of MMP-9 is upregulated by both 100 and 200 µg/mL LDL, depending on its oxidation state, at 24 h, compared to reagent blanks and media controls, but is highly variably at 48 h of incubation (**Figure 4(A)**), which may be caused by translation of MMP-9 mRNA. MMP-9 protein expression, in both cell lysates and secreted form in cultured supernatant of the macrophage foam cells induced by LDL, mm-LDL or ox-LDL, was then examined.

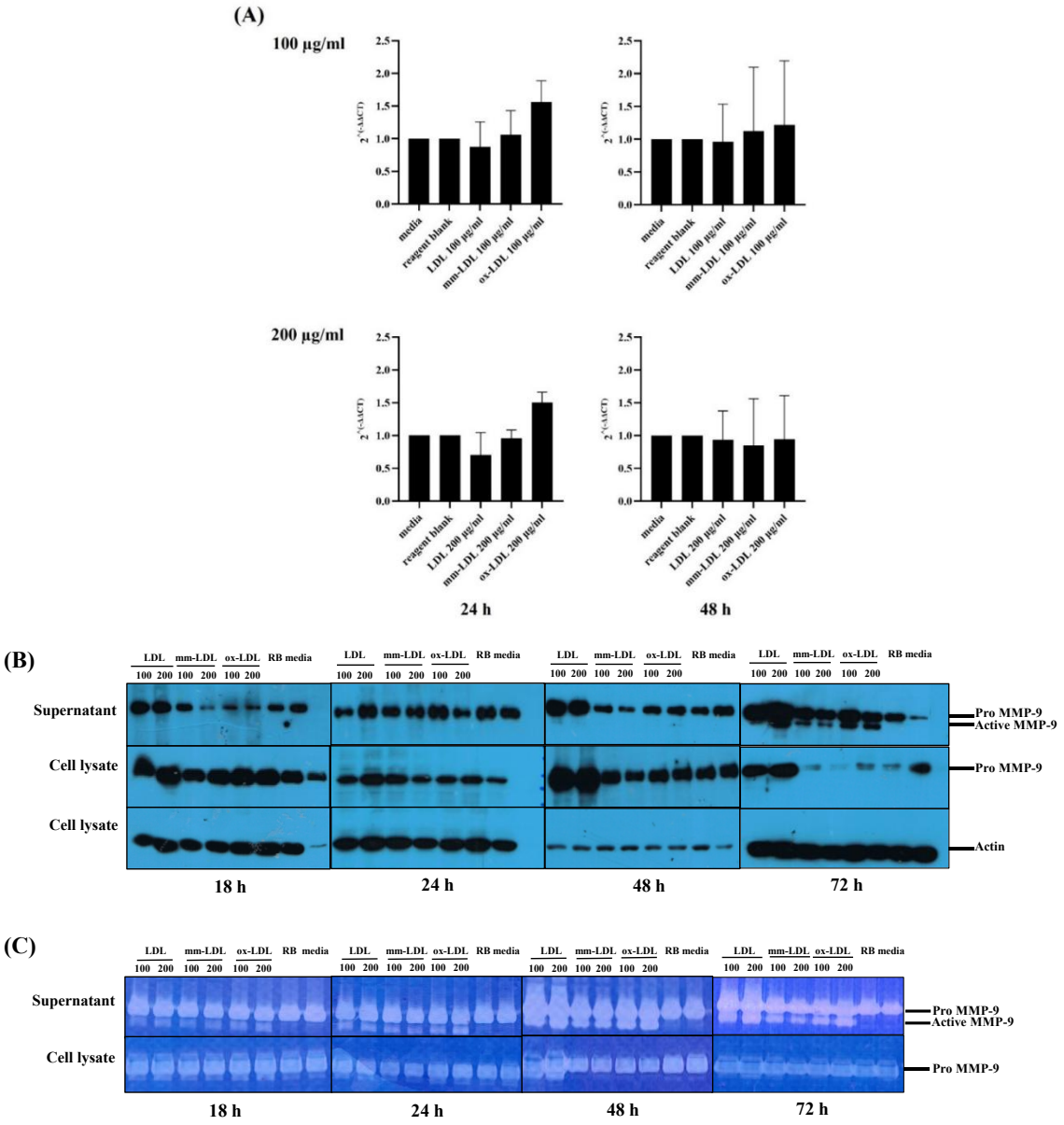

Figure 4 MMP-9 expression at the mRNA and protein levels. PMA-derived macrophages were co-cultivated without or with LDL, mm-LDL or ox-LDL at different concentrations and times. MMP-9 mRNA expression was determined by semi-quantitative RT-PCR (A), and high variation was found, reflecting the gene translation. The data represents the means ± SD of 3 independent experiments. MMP-9 expression at protein level and its activity were shown by Western blot analysis (B) and gelatin zymography (C), respectively, indicating that LDL and ox-LDL produce the largest induction of MMP-9 expression and activation. These results are representative of 3 independent experiments.

The results indicated that the pro-form of MMP-9 (MW 92 kDa) was found constitutively both in cell lysates and in culture supernatants under all conditions and tended to increase at 48 h. After 72 h of incubation, the level of MMP-9 expression in cell lysates was dramatically decreased whereas the secreted form in

cultured supernatant was increased. Furthermore, the active form of MMP-9 (MW 72 kDa) was clearly observed at this time point when various types of LDL were added into the macrophage cells, compared to the reagent blank and media control (**Figure 4(B)**). The highest expression of both pro- and active forms was induced by LDL, followed by ox-LDL, while mm-LDL induced the lowest level of MMP-9 expression. Gelatin zymography assays revealed that the enzymic activity of MMP-9 or gelatinase-B was correlated with the protein expression detected by Western blotting, shown in **Figure 4(B)**. Constant enzymic activity of pro-MMP-9 was seen in the cell lysate fraction under each incubation condition, whereas the enzymic activity of both pro- and active forms of MMP-9 in culture supernatant was increased in a time-dependent manner, compared to the reagent blank and media control, especially at 48 and 72 h. According to the results, the best inducer of MMP-9 expression and its enzymatic activity was LDL, followed by ox-LDL and mm-LDL (**Figure 4**). This correlates with the total cholesterol concentration in macrophages, the highest concentration being induced by LDL, followed by ox-LDL and mm-LDL (**Figure 2**). The gelatin zymographic analysis showed gradual transformation of the MMP-9 from the pro-form to the active form during prolonged incubation of macrophages with different types of LDL (**Figure 4(C)**), which may imply that during the longer period, foam cells derived from all types of LDL are involved in plaque instability at different levels determined by secretion of MMP-9.

Cell surface expression of CD147 expression on PMA-derived macrophages induced by both non-oxidized and oxidized LDL

CD147, an extracellular matrix metalloproteinase inducer (EMMPRIN), is known to be involved in induction of MMP-9 by macrophage upon foam cell formation [28,29]. Moreover, high-throughput compound screening revealed that ox-LDL-induced CD147 upregulation in macrophages was achieved through PI3K/Akt/mTOR signaling [22]. We therefore investigated whether different degrees of oxidation of LDL and the time of exposure affected the expression of this molecule. Anti-CD147 mAb was used to tag the molecule and was analyzed by flow cytometry. The results showed gradual, time-dependent upregulation of the membrane form of CD147 (mCD147) by all types of LDL, with a significant increase, compared to the reagent blank and media controls, after 72 h of incubation (**Figure 5**). Contradictory to results in the previous report [22], we found that at this point the expression level was reduced as the degree of oxidation of LDL increased. Additionally, the results revealed the correlation between the significant upregulation of membrane-bound CD147 (mCD147) shown (**Figure 5**), with the highest expression of MMP-9 and its conversion from pro-form to active form at 72 h of incubation by induction of all types of LDL, particularly LDL itself. It was previously reported that ox-LDL induced shedding of the mCD147 of lipid-loaded macrophages in a soluble form (sCD147), which then upregulated expression of MMP-9 and MMP-2 [30]. We found the greatest up-regulation of both MMP-9 and mCD147 when the macrophage foam cells were induced by non-oxidized LDL. Here we provide evidence that up-regulation of mCD147 by non-oxidized LDL could enhance MMP-9 production in this study model, compared to other oxidized forms of LDL.

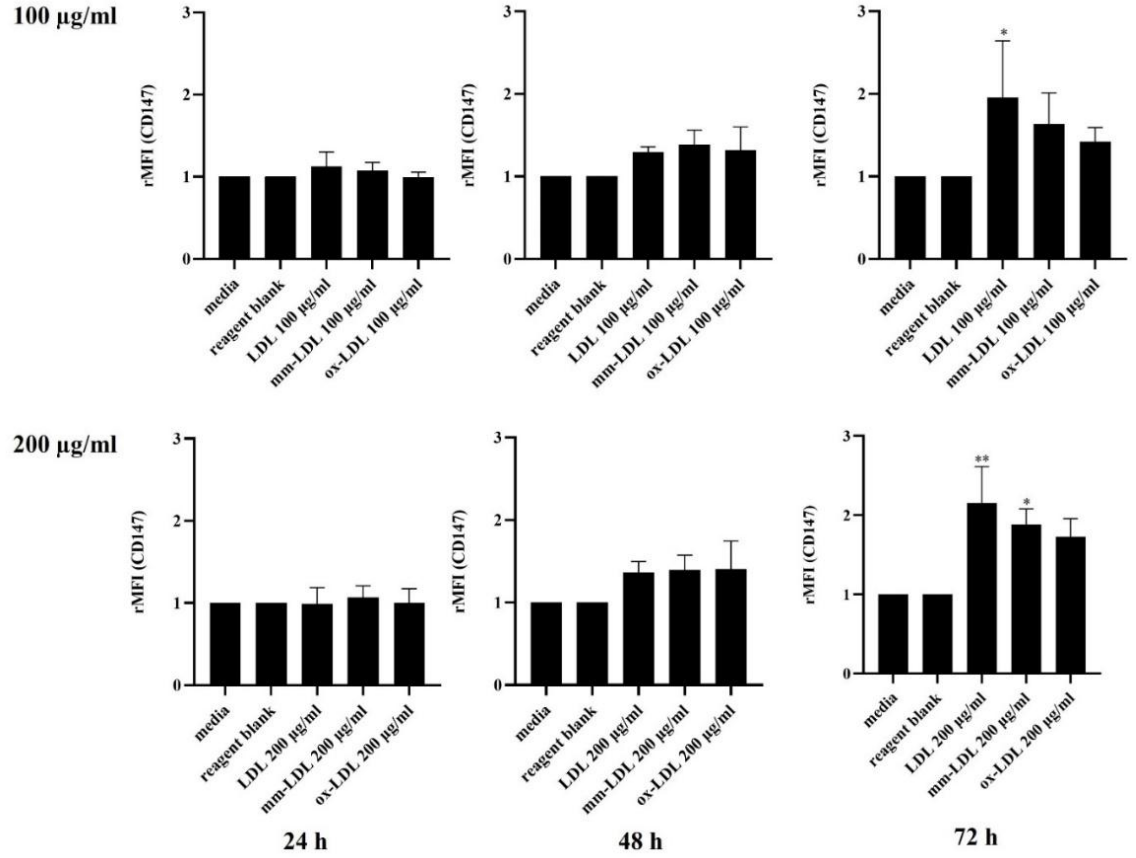

Figure 5 Membrane CD147 expression in PMA-derived macrophages. Macrophages were incubated without or with LDL, mm-LDL or ox-LDL at various concentrations for 24, 48 or 72 h. The cells were immunofluorescence-stained using anti-CD147 mAb. AF-488-anti-mIgs (dilution 1:500) was used as the secondary antibody and analyzed by flow cytometry. All types of LDLs produced significant increases in mCD147 expression compared to the reagent blank and media controls, after 72 h of incubation. Expression levels are shown as relative mean fluorescence intensity. Data represent means ± SD of 3 independent experiments (* indicated $p < 0.05$ and ** indicated $p < 0.01$).

Conclusions

This study revealed that all types of LDL can induce foam cell formation in a dose- and time-dependent manner, and notably that LDL shows strong induction of foam cell formation, among others, as shown in **Figure 2**. Although a previous report revealed that CD36 does not typically bind to native LDL with high affinity, but more prominently to modified forms, either mm-LDL and ox-LDL [14,31], this study reveals that CD36 plays a major role as an endocytic route for all LDL types studied. Furthermore, LDL upregulated expression of the pro-form of MMP-9 in macrophages, both in cell lysates and as the secreted form in the supernatant after 48 h of cultivation. Up-regulation and conversion of MMP-9 from the pro- to the active form were observed after 72 h of cultivation with all types of LDL. Notably, LDL elicited a more substantial induction response compared to ox-LDL, which correlated with the up-regulation of mCD147 in the macrophages studied (**Figure 5**). Based on our discovery, the strong induction of MMP-9 and mCD147 by LDL suggests that increasing plasma LDL, without extensive oxidation, can lead to atherogenesis and plaque destabilization. Moreover, CD147 can serve as a biomarker for the unstable atherosclerotic plaque condition, through its induction of MMP-9 expression. Additionally, elevated expression of CD36 and CD147 are critical drivers of LDL uptake and MMP-9 activation that contribute to foam cell accumulation and plaque destabilization, highlighting them as potential targets for reduction of foam cell formation or plaque rupture in cardiovascular diseases.

Acknowledgements

This research was supported by 1) Suranaree University of Technology (SUT), Thailand, 2) Thailand Science Research and Innovation (TSRI), and 3) National Science, Research and Innovation Fund (NSRF) (NRIIS No.195613 and No. 204203) and Biochemistry and Electrochemistry Research Unit grant. The authors express their thanks to Dr. David Apps, Biochemistry Reader, School of Biomedical Sciences, Edinburgh University, Scotland, for his critical manuscript reading and language improvements.

Ethics approval

The study was conducted in accordance with the guidelines for human handling based on the declaration of Helsinki. The documentation required for human studies was approved by the Ethics committee for Researchers Involving Human subjects, Suranaree University of Technology, Nakhon Ratchasima, Thailand on June15th, 2022.

Declaration of Generative AI in Scientific Writing

No content generation or data interpretation was performed by AI. The authors take full responsibility for the content and conclusions of this work

CRediT Author Statement

Kanokwan Lowhalidanon: Methodology experimental and formal analysis, Writing original draft. **Warapan Panchai:** CD147 experiment and RT-qPCR, data curation. **Panida Khunkaewla:** Supervision, conceptualization, validation, Writing - reviewing and editing.

References

[1] AV Poznyak, NG Nikiforov, AM Markin, DA Kashirskikh, VA Myasoedova, EV Gerasimova and AN Orekhov. Overview of OxLDL and its impact on cardiovascular health: Focus on atherosclerosis. *Frontiers in Pharmacology* 2020; **11**, 613780.

[2] A Ijaz, B Yarlagadda and M Orecchioni. Foamy macrophages in atherosclerosis: Unraveling the balance between pro- and anti-inflammatory roles in disease progression. *Frontiers in Cardiovascular Medicine* 2025; **12**, 1589629.

[3] JLM Björkegren and AJ Lusis. Atherosclerosis: Recent developments. *Cell* 2022; **185(10)**, 1630-1645.

[4] H Itabe, T Obama and R Kato. The dynamics of oxidized LDL during atherogenesis. *Journal of Lipids* 2011; **2011**, 418313.

[5] K Lowhalidanon and P Khunkaewla. Discrimination between minimally modified LDL and fully oxidized LDL using monoclonal antibodies. *Analytical Biochemistry* 2021; **619**, 114103.

[6] H Itabe, N Sawada, T Makiyama and T Obama. Structure and dynamics of oxidized lipoproteins *in vivo*: Roles of high-density lipoprotein. *Biomedicines* 2021; **9(6)**, 655.

[7] JL Goldstein and MS Brown. The LDL receptor. *Arteriosclerosis, Thrombosis, and Vascular Biology* 2009; **29(4)**, 431-438.

[8] CNJ Kzhyshkowskaa and S Gordon. Role of macrophage scavenger receptors in atherosclerosis. *Immunobiology* 2012; **217(5)**, 492-502.

[9] H Jiang, Y Zhou, SM Nabavi, A Sahebkar, PJ Little, S Xu, J Weng and J Ge. Mechanisms of oxidized LDL-mediated endothelial dysfunction and its consequences for the development of atherosclerosis. *Frontiers in Cardiovascular Medicine* 2022; **9**, 925923.

[10] JFC Glatz, M Nabben and JJFP Luiken. CD36 (SR-B2) as master regulator of cellular fatty acid homeostasis. *Current Opinion in Lipidology* 2022; **33(2)**, 103-111.

[11] E Vassiliou and R Farias-Pereira. Impact of lipid metabolism on macrophage polarization: Implications for inflammation and tumor immunity. *International Journal of Molecular Sciences* 2023; **24(15)**, 12032.

[12] Z Song, H Xia, L Yang, S Wang and G Sun. Lowering the n-6/n-3 PUFAs ratio inhibits the formation of THP-1 macrophage-derived foam cell. *Lipids in Health and Disease* 2018; **17(1)**, 125.

[13] MTL Lhoëst, A Martinez, L Claudi, E Garcia, A Benitez-Amaro, A Polishchuk, J Piñero, D Vilades, JM Guerra, F Sanz, N Rotllan, JC Escolà-Gil and V Llorente-Cortés. Mechanisms modulating foam cell formation in the arterial

intima: Exploring new therapeutic opportunities in atherosclerosis. *Frontiers in Cardiovascular Medicine* 2024; **11**, 1381520.

[14] M Rac. Human CD36: Gene regulation, protein function, and its role in atherosclerosis pathogenesis. *Genes* 2025; **16(6)**, 705.

[15] HF Bakheit, S Taurin, EM Elamin and M Bakhiet. Akt1 players promote PMA U937 cell line differentiation into macrophage-like cells. *Arab Gulf Journal of Scientific Research* 2024; **42(4)**, 1257-1270.

[16] YG Chen, XJ Zhang, SB Huang and M Febbraio. Hidden features: CD36/SR-B2, a master regulator of macrophage phenotype/function through metabolism. *Frontiers in Immunology* 2024; **15**, 1468957.

[17] S Gencer, BR Evans, EPCVD Vorst, Y Döring and C Weber. Inflammatory chemokines in atherosclerosis. *Cells* 2021; **10(2)**, 226.

[18] C Qian, X You, B Gao, Y Sun and C Liu. The role of ROS in atherosclerosis and ROS-based nanotherapeutics for atherosclerosis: Atherosclerotic lesion targeting, ROS scavenging, and ROS-responsive activity. *ACS Omega* 2025; **10(22)**, 22366-22381.

[19] I Jansen, R Cahalane, R Hengst, A Akyildiz, E Farrell, F Gijsen, E Aikawa, KVD Heiden and T Wissing. The interplay of collagen, macrophages, and microcalcification in atherosclerotic plaque cap rupture mechanics. *Basic Research in Cardiology* 2024; **119(2)**, 193-213.

[20] GM Sanda, M Deleanu, L Toma, CS Stancu, M Simionescu and AV Sima. Oxidized LDL-exposed human macrophages display increased MMP-9 expression and secretion mediated by endoplasmic reticulum stress. *Journal of Cellular Biochemistry* 2017; **118(4)**, 661-669.

[21] R Asgari, A Vaisi-Raygani, MSE Aleagha, P Mohammadi, M Bakhtiari and N Arghiani. CD147 and MMPs as key factors in physiological and pathological processes. *Biomedicine and Pharmacotherapy* 2023; **157**, 113983.

[22] JJ Lv, H Wang, HY Cui, ZK Liu, RY Zhang, M Lu, C Li, YL Yong, M Liu, H Zhang, TJ Zhang, K Zhang, G Li, G Nan, C Zhang, SP Guo, L Wang, ZN Chen and H Bian. Blockade of macrophage CD147 protects against foam cell formation in atherosclerosis. *Frontiers in Cell and Developmental Biology* 2021; **8**, 609090.

[23] MG Song, IG Ryoo, HY Choi, BH Choi, ST Kim, TH Heo, JY Lee, PH Park and MK Kwak. NRF2 signaling negatively regulates Phorbol-12-Myristate-13-Acetate (PMA) induced differentiation of human monocytic U937 cells into pro-inflammatory macrophages. *Plos One* 2015; **10(7)**, e0134235.

[24] T Sritrakarn, K Lowhalidanon and P Khunkaewla. CDR identification, epitope mapping and binding affinity determination of novel monoclonal antibodies generated against human apolipoprotein B-100. *BBA: Proteins and Proteomics* 2025; **1873**, 141058.

[25] T Miyazaki. Pinocytotic engulfment of lipoproteins by macrophages. *Frontiers in Cardiovascular Medicine* 2022; **9**, 957897.

[26] JFC Glatz and J Luiken. Dynamic role of the transmembrane glycoprotein CD36 (SR-B2) in cellular fatty acid uptake and utilization. *Journal of Lipid Research* 2018; **59(7)**, 1084-1093.

[27] L Lu, J Huang, X Xue, T Wang, Z Huang and J Li. Berberine regulated miR150-5p to inhibit P2X7 receptor, EMMPRIN and MMP-9 expression in oxLDL induced macrophages. *Frontiers in Pharmacology* 2021; **12**, 639558.

[28] DM Tanase, E Valasciuc, IB Anton, EM Gosav, N Dima, AI Cucu, CF Costea, DE Floria, LL Hurjui, CC Tarniceriu, M Ciocoiu and M Floria. Matrix metalloproteinases: Pathophysiologic implications and potential therapeutic targets in cardiovascular disease. *Biomolecules* 2025; **15(4)**, 598.

[29] T Li, X Li, Y Feng, G Dong, Y Wang and J Yang. The role of matrix metalloproteinase-9 in atherosclerotic plaque instability. *Mediators of Inflammation* 2020; **2020**, 3872367.

[30] HH Yue, N Leng, ZB Wu, HM Li, XY Li and P Zhu. Expression of CD147 on phorbol-12-myristate-13-acetate (PMA)-treated U937 cells differentiating into foam cells. *Archives of Biochemistry and Biophysics* 2009; **485(1)**, 30-34.

[31] K Tian, Y Xu, A Sahebkar and S Xu. CD36 in atherosclerosis: Pathophysiological mechanisms and therapeutic implications. *Current Atherosclerosis Reports* 2020; **22(10)**, 5.

Supplementary Material

1) Assessment of the degree of LDL oxidation

LDL oxidation was performed using 10 µM $CuSO_4$ as an oxidizing agent for 9 and 48 h to generate mm-LDL and ox-LDL, respectively, as described in Materials and Methods. The degree of oxidation of LDL was evaluated according to a previous report by a thiobarbituric acid-reactive substance (TBARS) assay and indirect ELISA using in-house anti-human LDL mAb clones hLDL-E8 and hLDL-2D8 [1]. The results showed that the degree of lipid oxidation determined by TBARS increased when LDL was oxidized and reached a maximum after 9 h. On prolonged incubation for 48 h there was no significant increase in lipid oxidation (**Figure S1(A)**), but indirect ELISA using both anti-human LDL mAb clone hLDL-E8 (**Figure S1(B)**) and hLDL-2D8 (**Figure S1(C)**) showed that the binding efficiency decreased significantly after 48 h of incubation, reflecting the oxidative modification of LDL protein apoB-100. These results suggested that mm-LDL and ox-LDL were successfully generated and could be used in the experiments.

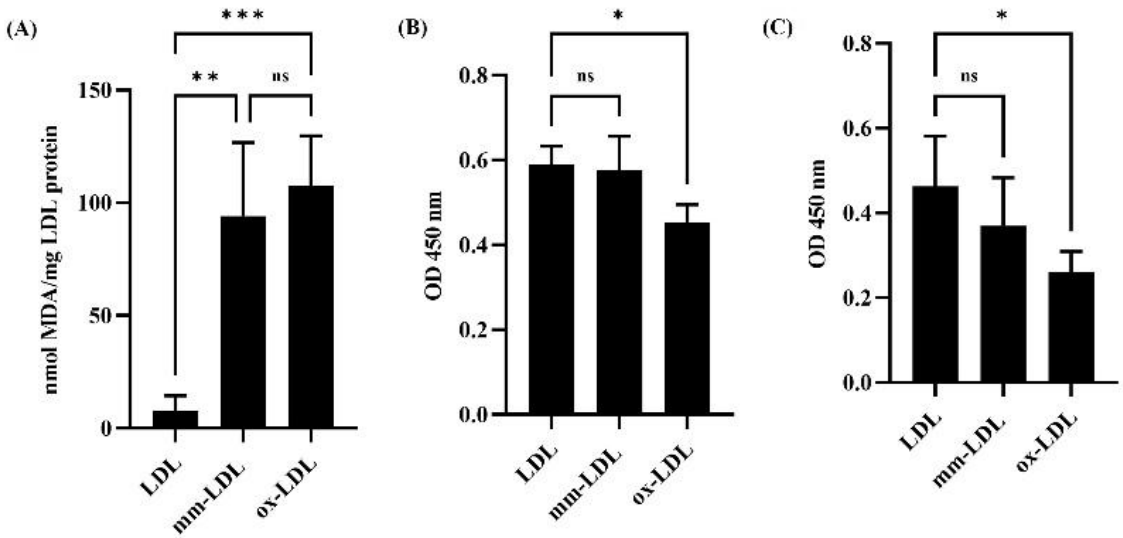

Figure S1 Assessment of the degree of LDL oxidation. The degree of LDL oxidation was assessed by a thiobarbituric-acid reactive substance (TBARS) assay (A) and indirect ELISA using in-house anti-human LDL clone hLDL-E8 (B) and hLDL-2D8 (C) for the oxidative modification of the lipid and protein respectively. The data represent the mean ±SD of four independent experiments (ns indicates not significant, * indicates $p < 0.05$, ** indicates $p < 0.01$, and *** indicates $p < 0.001$).

2) Cell surface expression of LDL-receptor (LDL-R), CD36 and CD147

PMA-derived macrophages were co-cultivated with different types of LDL at final concentrations of 100 and 200 µg/mL for 24, 48 and 72 h. The cells were subjected to indirect immunofluorescence staining and flow cytometry analysis according to Materials and Methods. Histograms of LDL receptor (LDL-R), CD36 and CD147 expression are shown in **Figures S2 - S4** respectively.

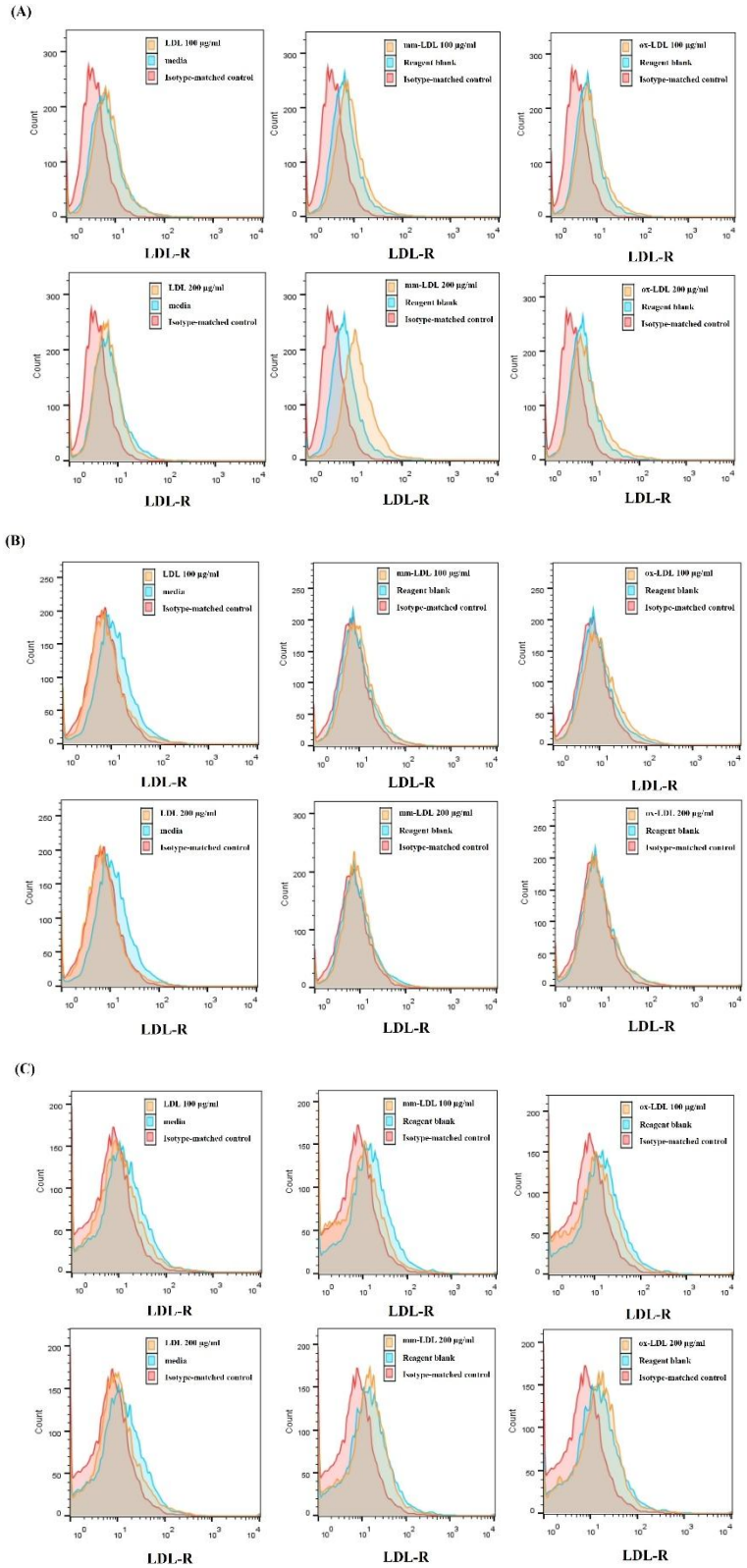

Figure S2 Expression of LDL-receptor (LDL-R). PMA-derived macrophages were co-cultivated with different types of LDL at final concentrations of 100 and 200 µg/mL for 24 h (A), 48 h (B) and 72 h (C). The cells were subjected to indirect immunofluorescence staining and flow cytometry analysis. Histograms show the expression of LDL-R on the cell surface under each condition compared to a medium control for LDL-incubated macrophages, or reagent blank for oxidized-LDL incubated macrophages, and isotype-matched control. A representative result from one of three independent experiments is shown.

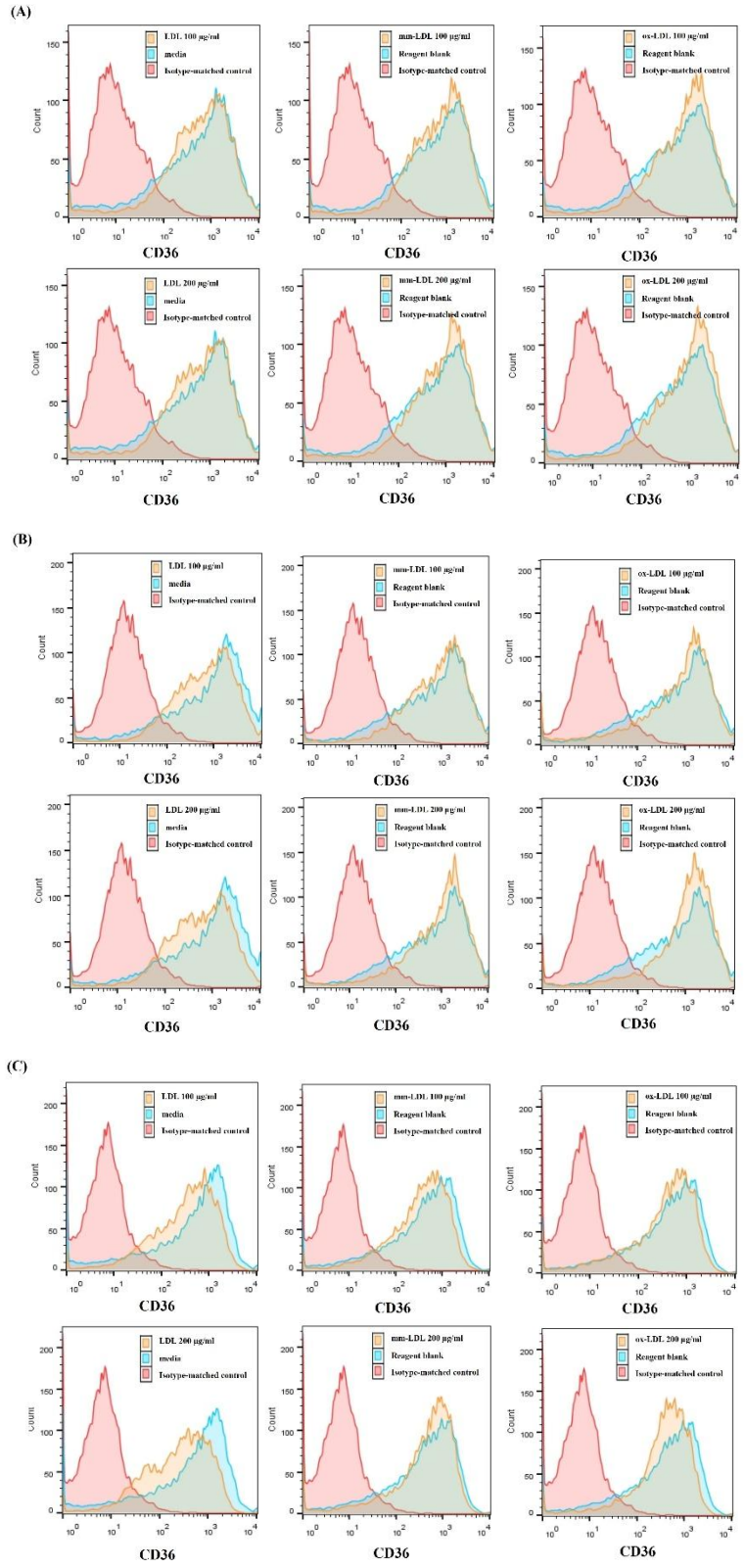

Figure S3 Expression of CD36. PMA-derived macrophages were co-cultivated with different types of LDL at final concentrations of 100 and 200 μg/mL for 24 h (A), 48 h (B) and 72 h (C). The cells were subjected to indirect immunofluorescence staining and flow cytometry analysis. Histogram shows the expression of CD36 on the cell surface under each condition compared to a media control for LDL incubated macrophages, or reagent blank for oxidized-LDL incubated macrophages, and isotype-matched control. A representative result from one of three independent experiments is shown.

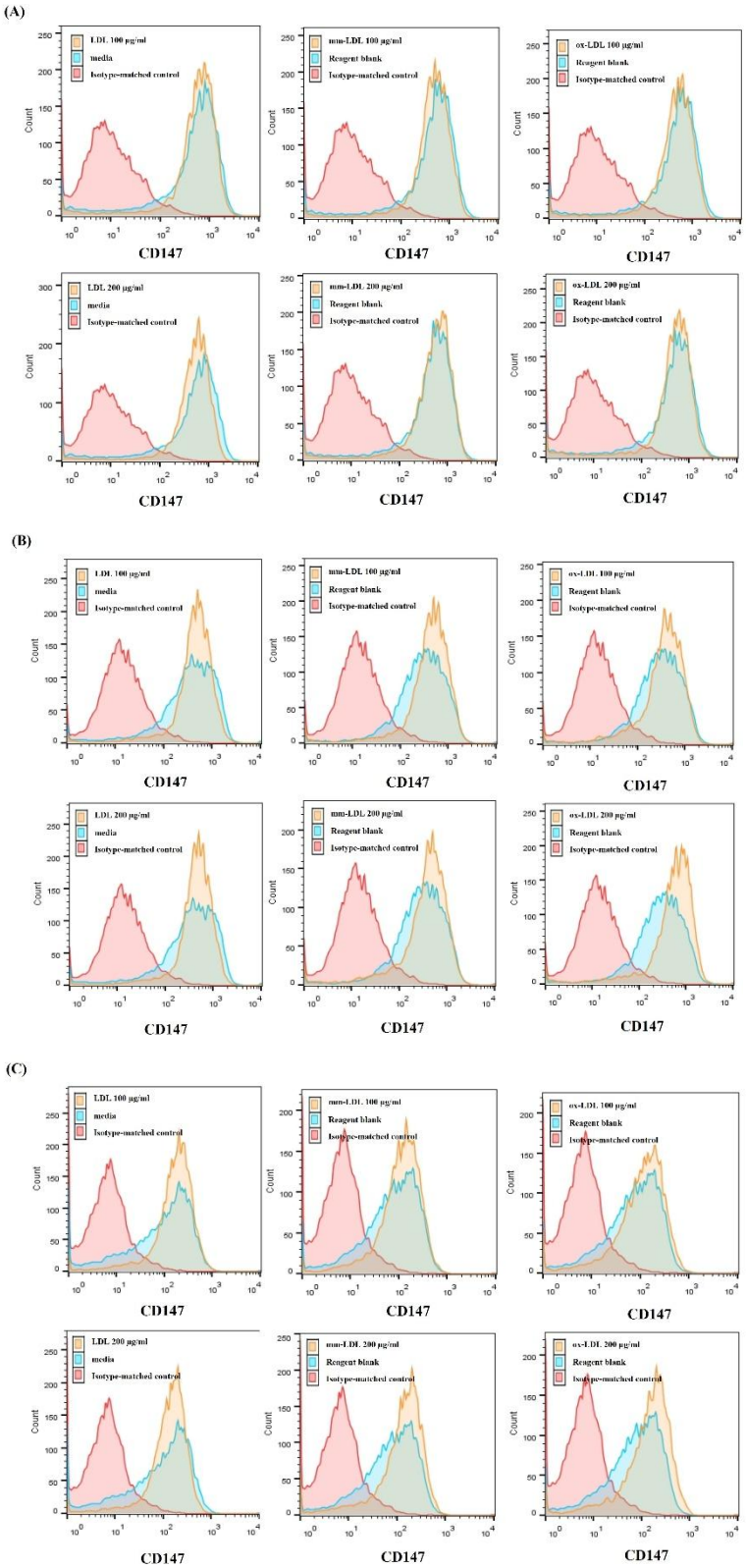

Figure S4 Expression of CD147. PMA-derived macrophages were co-cultivated with different types of LDL at final concentrations of 100 and 200 μg/mL for 24 h (A), 48 h (B) and 72 h (C). The cells were subjected to indirect immunofluorescence staining and flow cytometry analysis. Histograms show the expression of mCD147 on the cell surface under each condition compared to a medium control for LDL incubated macrophages, or reagent blank for oxidized-LDL incubated macrophages, and isotype-matched control. A representative result from one of three independent experiments is shown.

3) Raw data for Western blot and gelatin zymography

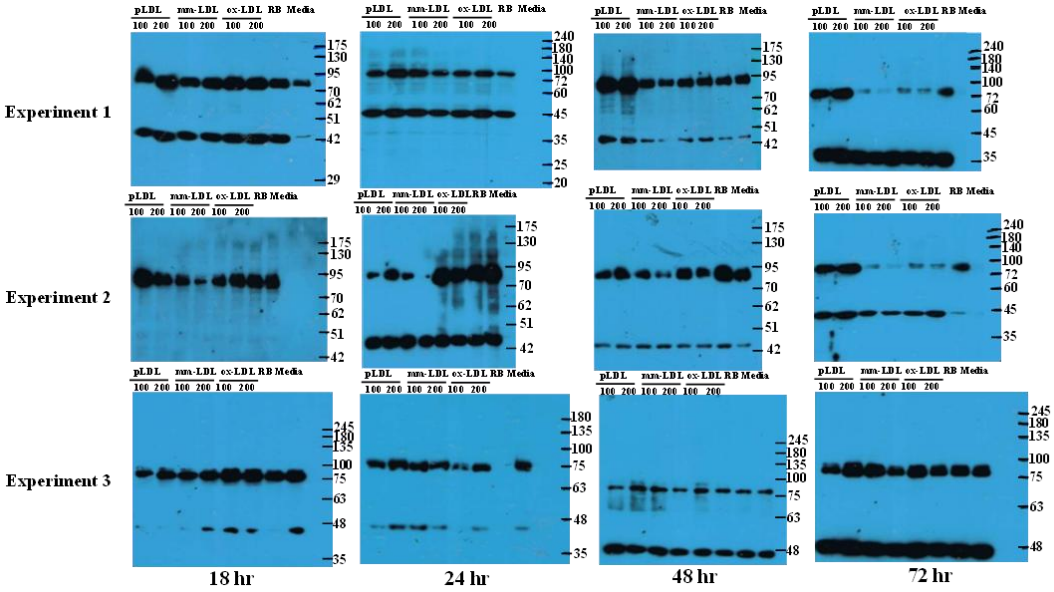

(A)

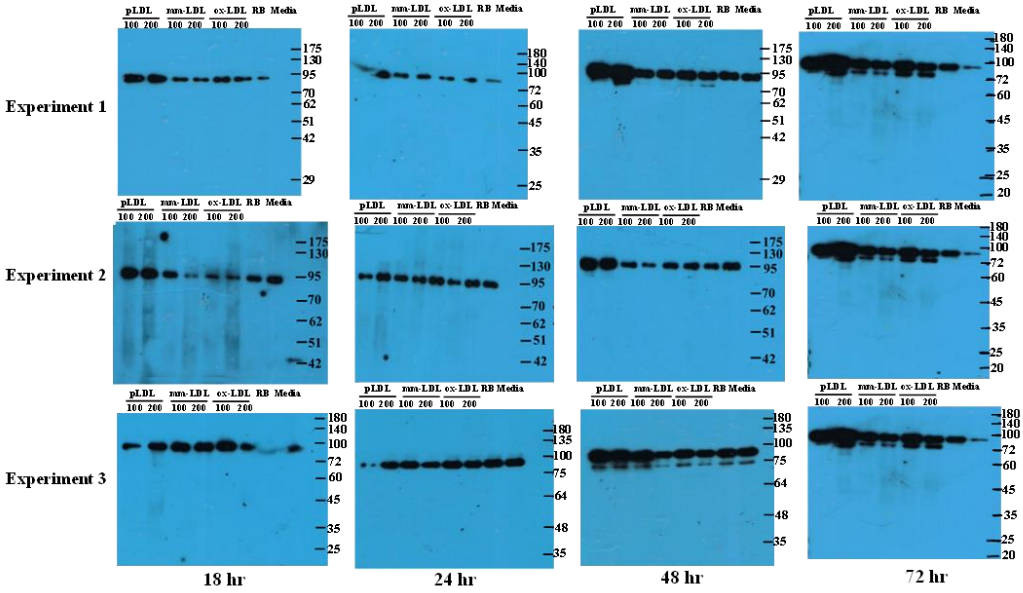

(B)

Figure S5 An equal amount of protein, either 6 µg of cell lysates (A) or 200 µg of cultured supernatant (B) was electro-separated using 10% SDS-PAGE under reducing conditions and electro-transferred onto PVDF membrane. The membranes were subjected to Western blotting using MMP-9 mAb (Invitrogen, USA) at a dilution of 1:2000 as a primary antibody (mAb against beta-actin (Bio-Rad, USA) at a dilution 1:40000 was used to as loading control for cell lysates analysis) and rabbit anti-mouse HRP-Igs at a dilution 1:5000 was used as the secondary antibody. The protein bands were visualized using a chemiluminescence detection system.

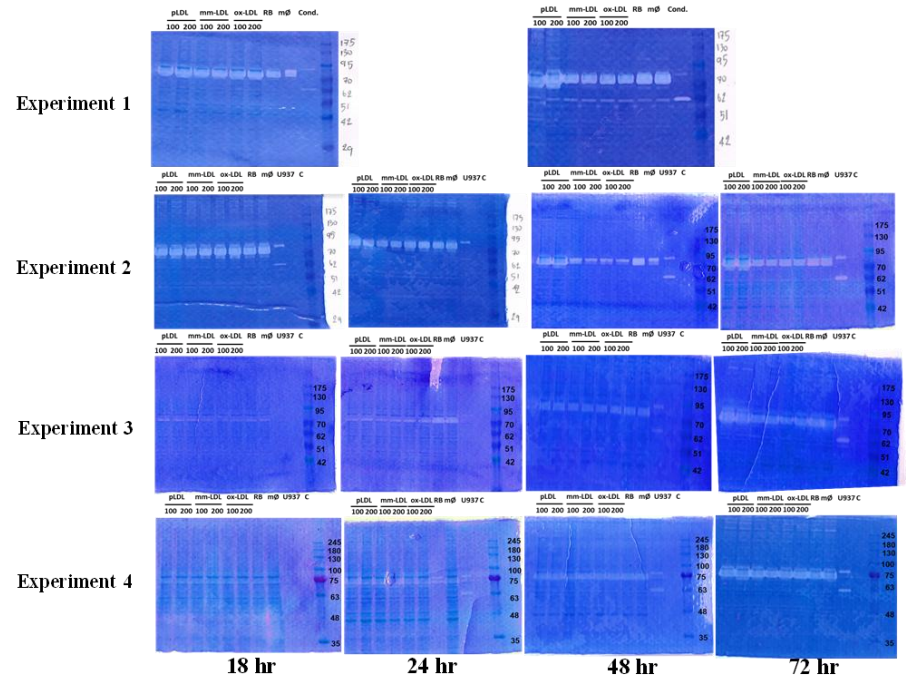

(A)

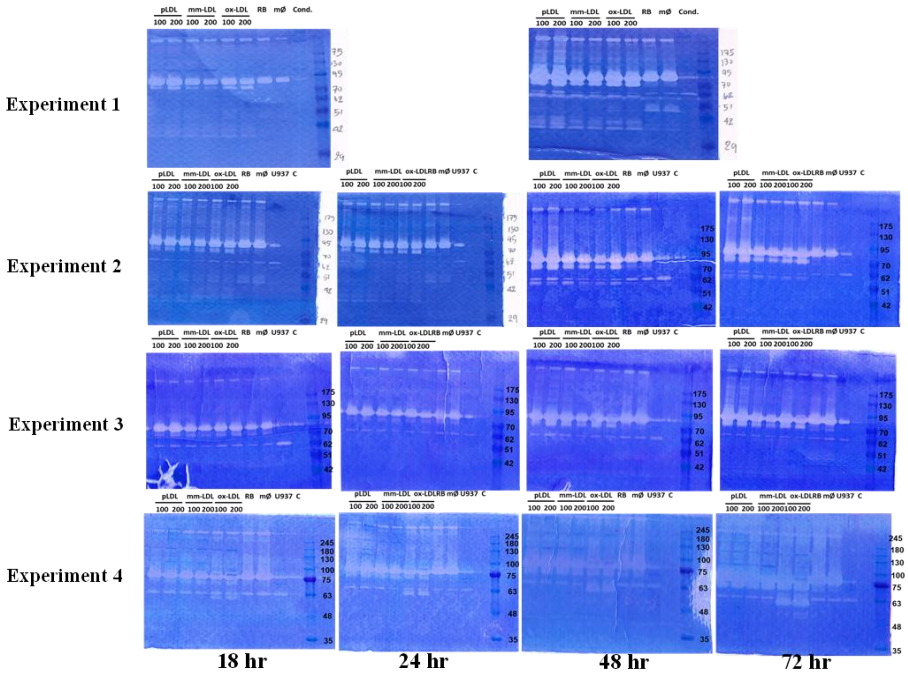

(B)

Figure S6 An equal amount of protein, either 6 µg of cell lysates (A) or 200 µg of cultured supernatant (B), was electro-separated using 10% SDS-PAGE containing 0.1% gelatin under non-reducing condition at 150 volts for 1.5 h. The isolated proteins were re-natured using re-naturing buffer containing 2.5% Triton X-100® for 40 min at RT and subsequently incubated in activation buffer (50 mM Tris-HCl, 0.15 M NaCl, and 10 mM $CaCl_2$) at 37 °C for 18 h before staining with Coomassie Brilliant Blue R250. The clear zones of hydrolytic activity of Pro-MMP-9 (92 kDa), active MMP-9 (83 kDa) Pro-MMP-2 (72 kDa) and Active MMP-2 (63 kDa) were observed. (Cond = media control).

Reference

[1] K Lowhalidanon and P Khunkaewla. Discrimination between minimally modified LDL and fully oxidized LDL using monoclonal antibodies. *Analytical Biochemistry* 2021; **619**, 114103.